

LncRNA-GAS5 Inhibits Expression of miR-103 and Ameliorates the Articular Cartilage in Adjuvant-Induced Arthritis in Obese Mice

Hongwei Chen^{1,2}, Chuan He^{1,2}, Yan Liu², Xiaolin Li², Chaoju Zhang², Qunyan Qin², and Qixiong Pang² 

Abstract

We explored whether long noncoding RNA growth arrest-specific transcript 5 (LncRNA-GAS5) small interfering RNA (siRNA) reduced cartilage destruction in obese mice with adjuvant-induced arthritis. We studied the effects of LncRNA-GAS5 siRNA on the polyarthritis index; hind paw swelling; and the serum levels of certain biochemicals, cytokines, and oxidative stress parameters. We measured the expression levels of matrix metalloproteinases (MMP)-13, NF- κ B, fibroblast growth factor (FGF) 21, p38, Akt, and PI3K in cartilage via Western blotting and quantitative reverse transcription PCR. Long noncoding RNA-GAS5 siRNA reduced joint swelling; the serum levels of arthritis-associated biochemicals, cytokines, and oxidative stress markers; and cartilage MMP-13, NF- κ B, FGF21, p38, Akt, and PI3K levels. Cartilage miR-103 expression was reduced. Histopathologically, LncRNA-GAS5 siRNA ameliorated the pathological changes of cartilage. Long noncoding RNA-GAS5 siRNA prevented cartilage destruction by inhibiting miR-103 expression.

Keywords

cartilage, inflammation, LncRNA-GAS5 miR-103, rheumatoid arthritis

Introduction

Rheumatoid arthritis (RA) is an autoimmune disorder associated with progressive joint degeneration¹ characterized by osteophyte formation, loss of articular cartilage, and extracellular matrix degradation.² Rheumatoid arthritis causes global disability. The etiopathogenesis is incompletely known but increases in the levels of growth factors, chemokines, and cytokines, and changes in synovial factor (SF) levels are involved.³ Increased SF levels enhance the secretion of matrix metalloproteinases (MMPs) and mediators of inflammation.⁴ Bone degeneration reflects changes in the ratios of osteoclasts to osteoblasts⁵ and chronic inflammation develops.⁶ In obese patients, the levels of pro-inflammatory cytokines rise and those of anti-inflammatory cytokines fall.⁷ Fibroblast growth factor (FGF) triggers differentiation of white to brown adipose tissue, further enhancing obesity⁸; thus, FGF may be a useful therapeutic target.⁹ Conventional therapies are inadequate, and RA remains poorly managed.

Long noncoding RNAs (LncRNAs) are noncoding RNAs longer than 200 nucleotides. The growth arrest-specific transcript 5 (GAS5) gene suppresses tumor growth; LncRNA-GAS5 suppresses cell proliferation of prostate, colorectal, and

bladder cancers.¹⁰ LncRNA-GAS5 reduces miR-23a expression, thereby protecting against hepatic fibrosis by attenuating the PTEN/PI3K/Akt pathway.¹¹ Long noncoding RNA-GAS5 stimulates miR-103 expression, helping to prevent endometrial cancer.¹² miR-103 expression is enhanced in patients with osteoarthritis; modulation thereof prevents arthritis by reducing the levels of inflammatory mediators.¹³ We explored whether LncRNA-GAS5 small interfering RNA (siRNA) protected against RA.

¹ The Third Clinical Medical School, Yangtze University, Jingzhou, Hubei, China

² Department of orthopedics, Jingzhou Traditional Chinese Medicine Hospital, Jingzhou, Hubei, China

Received 10 March 2020; received revised 02 April 2020; accepted 01 June 2020

Corresponding Author:

Qixiong Pang, Department of orthopedics, Jingzhou Traditional Chinese Medicine Hospital, No. 172 Jiangjin East Road, Shashi District, Jingzhou, Hubei 434000, China.

Email: TheraArvinjSgRxW@yahoo.com



Materials and Methods

Animals

C57BL/6 mice (4 weeks old) were held under a 12-h/12-h light/dark cycle at $60\% \pm 5\%$ relative humidity and $24\text{ }^{\circ}\text{C} \pm 3\text{ }^{\circ}\text{C}$. All animals were fed 60 kcal of fat daily. All animal protocols were approved by the institutional animal ethical committee of Jingzhou Traditional Chinese Medicine Hospital, China (approval no. IAEC/JTCMH/2018/08).

Experimental

Thirty animals were divided into 3 of 10 groups (control, RA, and RA/LncRNA-GAS5). Rheumatoid arthritis was induced as previously described.¹⁴ Isometric incomplete Freund's adjuvant (IFA) was prepared via emulsification with 2 mL of bovine type II collagen solution and acetic acid, and 0.1 mL was injected for 3 weeks into the paw plantar surfaces of mice that weighed $>30\text{ g}$. Rheumatoid arthritis development was assessed by evaluating hind paw swelling. The siRNA targeting LncRNA-GAS5 was injected into the tail vein (25 nmol/kg) together with the Enttransfer-in vivo reagent according to the manufacturer's protocol on days 7 and 14, 30 minutes after IFA administration.

Estimation of the polyarthritis index and hind paw swelling. The polyarthritis indices and hind paw swelling were determined at the end of the experiment. Swelling was estimated using a volume displacement method and was scored as final paw volume/original volume. The polyarthritis index ranges from 0 to 4: 0—no swelling, 1—little erythema and slight edema, 2—erythema from the ankle to the tarsal bone and slight edema, 3—erythema from the ankle to the tarsal bone and moderate edema, 4—erythema and edema throughout the leg.

Estimation of biochemical parameters. Serum high-density lipoprotein (HDL), low-density lipoprotein (LDL), aspartate aminotransferase (AST), and alanine aminotransferase (ALT) levels were estimated using commercial kits following the manufacturer instructions. The quantitative turbidimetric test was used to estimate C-reactive protein (CRP) concentrations. Interleukin (IL)-17, IL-6, and IL-4 levels were estimated via commercial enzyme-linked immunosorbent assays (ELISAs) as per the manufacturer instructions.

Oxidative stress markers. Serum malondialdehyde (MDA), reduced glutathione (GSH), and superoxide dismutase (SOD) levels were estimated via commercial ELISAs as per the manufacturer instructions.

Immunohistochemistry. Cartilage IL-17 and FGF21 levels were measured immunohistochemically. Isolated cartilage was fixed in 10% (vol/vol) formalin, embedded in paraffin, sectioned at 5- μm thickness, and incubated for 60 minutes at $60\text{ }^{\circ}\text{C}$. Hydrogen peroxide was used to neutralize endogenous peroxidase activity. The sections were incubated overnight with antibodies against IL-17 and FGF21 diluted in phosphate-buffered saline.

The secondary antibody was horseradish peroxidase-labeled goat anti-rabbit IgG; the sections were incubated with this antibody for 60 minutes at room temperature. Diaminobenzidine was added, followed by counterstaining with hematoxylin. All sections were hydrated, sealed, and observed under an inverted microscope.

Real-time polymerase chain reaction analysis. Cartilage RNA was isolated using TRIzol reagent. A RevertAid First Strand cDNA Synthesis Kit (Fermentas) was used to reverse-transcribe RNA. The primers described below were mixed with RT2 SYBR Green Master Mix (Superarray) followed by Quantitative SYBR Green PCR.

Western blotting. Total proteins of cartilage were extracted into ice-cold radioimmunoprecipitation lysis buffer; the DC assay was used to estimate proteins that were then separated using 10% (wt/vol) sodium dodecyl sulphate polyacrylamide gel electrophoresis, transferred to polyvinylidene difluoride membranes, and blocked with 5% (wt/vol) fresh nonfat dry milk powder. The membranes were incubated at $4\text{ }^{\circ}\text{C}$ overnight with primary antibodies against MMP-13, NF- κB , FGF21, p38, Akt, PI3K, and β -actin and then with appropriate secondary antibodies for 60 minutes at room temperature. Chemiluminescence was used for band enhancement and ImageLab software (Bio-Rad) was used to perform densitometric analysis.

Histopathological analysis. Cartilage tissues were fixed in 10% (vol/vol) formalin, paraffinized, and sectioned at 5- μm thickness. The sections were stained for 5 minutes at $37\text{ }^{\circ}\text{C}$ with hematoxylin and washed for 10 minutes with water. Eosin (5% wt/vol) was added for 3 minutes followed by dehydration with alcohol. Histopathological changes were evaluated under a light microscope.

Statistical analysis. All data are shown as means \pm SE of the mean (SEM; $n = 10$). Results were compared using 1-way analysis of variance and the Dunnett post hoc test (GraphPad Prism ver. 6.1 software; GraphPad). P values $< .05$ were considered to be significant.

Results

Long Noncoding RNA-GAS5 siRNA Reduces the Polyarthritis Index and Hind Paw Swelling

Figure 1 shows the effect of LncRNA-GAS5 siRNA on the polyarthritis index and hind paw swelling. Both parameters were higher in RA than control mice but were reduced in RA mice by LncRNA-GAS5 siRNA treatment.

Long Noncoding RNA-GAS5 siRNA Normalizes Biochemical Parameters

The serum HDL level was lower in the RA than the control group but the levels of AST, ALT, LDL, and CRP were higher.

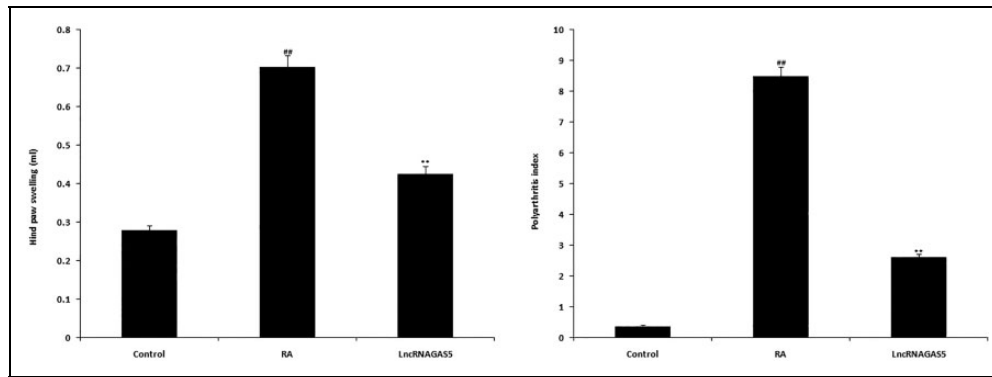


Figure 1. Effect of LncRNA-GAS5 siRNA on the polyarthrititis index and hind paw swelling. Mean \pm SEM (n = 10); ###P < .01 compared to controls; **P < .01 compared to the RA group. GAS5 indicates growth arrest-specific transcript 5; LncRNA, long noncoding RNA; RA, rheumatoid arthritis; siRNA, small interfering RNA.

Table 1. Effects of LncRNA-GAS5 siRNA on Serum Biochemical Parameters.^a

Sr. No.	Group	HDL (mg/dL)	LDL (mg/dL)	AST (U/L)	ALT (U/L)	CRP (mg/L)
1	Control	52.8 \pm 1.85	10.6 \pm 0.19	58.6 \pm 3.19	39.2 \pm 2.96	2.38 \pm 0.28
2	RA	36.2 \pm 0.94 ^b	41.62 \pm 1.62 ^b	132.4 \pm 11.7 ^b	76.9 \pm 5.64 ^b	11.58 \pm 0.86 ^b
3	LncRNA-GAS5 siRNA	47.1 \pm 1.36 ^c	16.29 \pm 0.48 ^c	74.9 \pm 6.28 ^c	52.6 \pm 3.27 ^c	5.39 \pm 0.42 ^c

Abbreviation: ALT, alanine aminotransferase; AST, aspartate aminotransferase; CRP, C-reactive protein; GAS5, growth arrest-specific transcript 5; HDL, high-density lipoprotein; LDL, low-density lipoprotein; LncRNA, long noncoding RNA; RA, rheumatoid arthritis; siRNA, small interfering RNA.

^aMean \pm SEM (n = 10).

^bP < .01 compared to the control group.

^cP < .01 compared to the RA group.

LncRNA-GAS5 siRNA reduced these levels in RA mice (Table 1).

Long Noncoding RNA-GAS5 Normalizes Cytokine Production

The serum levels of IL-4, IL-6, and IL-17 are shown in Figure 2; these were higher in RA than control mice, but LncRNA-GAS5 siRNA reduced these levels in RA mice.

Long Noncoding RNA-GAS5 Normalizes Oxidative Stress

Glutathione and SOD levels were lower in the RA group than the control group, but the MDA level was higher. Long noncoding RNA-GAS5 siRNA treatment of RA mice restored the levels of these markers to those of the control (Figure 3).

Long Noncoding RNA-GAS5 Normalizes IL-17 and FGF21 Expression Levels

Cartilage IL-17 and FGF21 levels were immunohistochemically analyzed. FGF21 expression was reduced and IL-17 expression enhanced in RA compared to control cartilage. Long noncoding RNA-GAS5 siRNA treatment of RA mice restored the levels to those of the control (Figure 4).

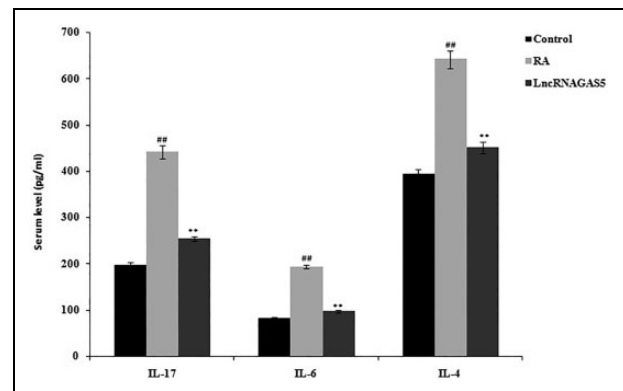


Figure 2. Effect of LncRNA-GAS5 siRNA on serum cytokine levels. Mean \pm SEM (n = 10); ###P < .01 compared to the control group; **P < .01 compared to the RA group. GAS5 indicates growth arrest-specific transcript 5; LncRNA, long noncoding RNA; RA, rheumatoid arthritis; siRNA, small interfering RNA.

Long Noncoding RNA-GAS5 Normalizes FGF21, MMP-13, and IL-17 Expression Levels

We used quantitative real-time polymerase chain reaction to assess the effect of LncRNA-GAS5 siRNA on the levels of cartilage mRNAs encoding FGF21, MMP-13, and IL-17 (Figure 5). Matrix metalloproteinases-13 and IL-17 expression increased and FGF-21 expression fell in the RA compared to the control group. Long noncoding RNA-GAS5 siRNA

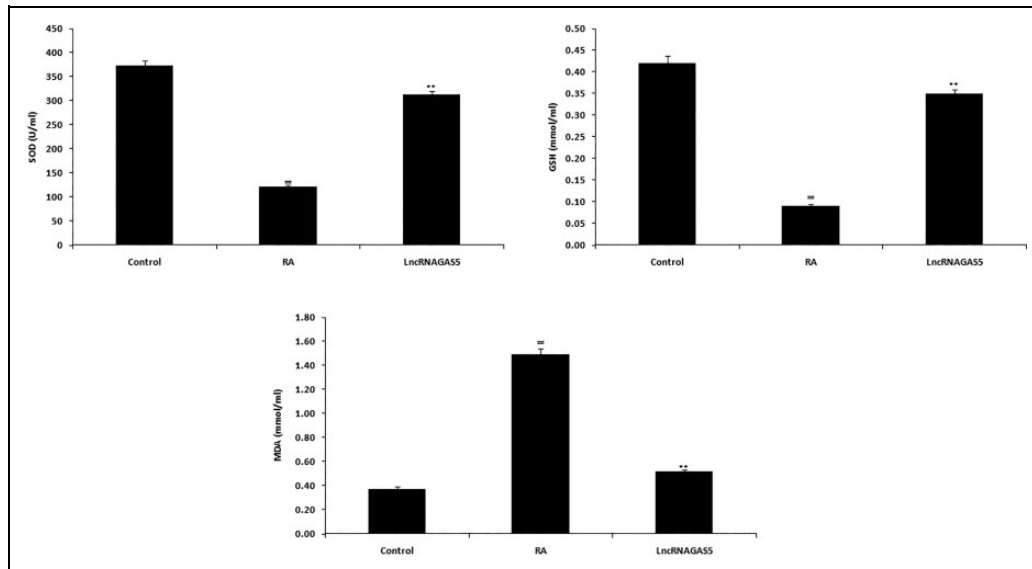


Figure 3. Effects of LncRNA-GAS5 siRNA on the levels of serum oxidative stress markers. Mean \pm SEM (n = 10); ###P < .01 compared to the control group; **P < .01 compared to the RA group. GAS5 indicates growth arrest-specific transcript 5; LncRNA, long noncoding RNA; RA, rheumatoid arthritis; siRNA, small interfering RNA.

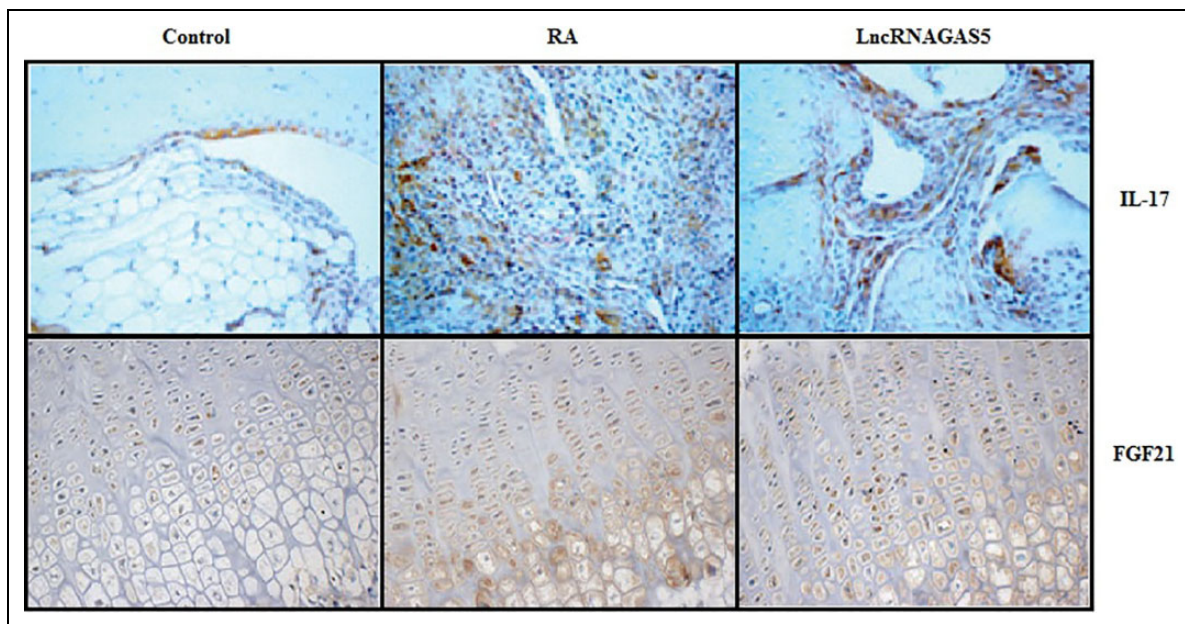


Figure 4. Effect of LncRNA-GAS5 siRNA on cartilage IL-17 and FGF21 expression levels. FGF indicates fibroblast growth factor; IL, interleukin; siRNA, small interfering RNA.

treatment of RA mice restored the levels to those of the control (Figure 5).

Long noncoding RNA-GAS5 siRNA Normalizes the Expression Levels of MMP-13, NF- κ B, FGF21, p38, Akt, and PI3K

The level of cartilage FGF-21 protein fell and those of MMP-13, NF- κ B, p38, Akt, and PI3K rose in the RA compared to the

control group. Long noncoding RNA-GAS5 siRNA normalized the expression levels of all proteins (Figure 6).

LncRNA-GAS5 siRNA Ameliorates miR-103 Underexpression

The cartilage miR-103 level was lower in the RA than the control group. However, LncRNA-GAS5 siRNA normalized miR-103 expression (Figure 7).

Long Noncoding RNA-GAS5 siRNA Ameliorates Histopathological Changes

Cartilage and bone damage, bone destruction, and pannus formation were evident in the RA group compared to the control group. Long noncoding RNA-GAS5 significantly reduced these pathologies (Figure 8).

Discussion

Rheumatoid arthritis is a chronic inflammatory autoimmune disease associated with synovial tissue destruction and bone damage.¹⁵ The available drugs are inadequate. We explored whether LncRNA-GAS5 siRNA protected against cartilage destruction in obese mice with adjuvant-induced arthritis. Long

noncoding RNA-GAS5 siRNA reduced the polyarthritis index and hind paw swelling, and normalized serum biochemical, cytokine, and oxidative stress parameters; cartilage MMP-13, NF- κ B, FGF21, p38, Akt, and PI3K protein levels; the miR-103 level; and histopathological changes. Rheumatoid arthritis is an inflammatory joint disorder; the polyarthritis index and hind paw swelling increase in animal models of RA,¹⁶ as we also found. Reductions in these parameters reduce cartilage injury¹⁷; LncRNA-GAS5 siRNA afforded such reductions. The increased serum cytokine levels in RA patients contribute to joint inflammation; anti-inflammatory drugs are used to manage RA.¹⁸ Long noncoding RNA-GAS5 siRNA reduced the serum cytokine level in RA mice. In obese subjects, white

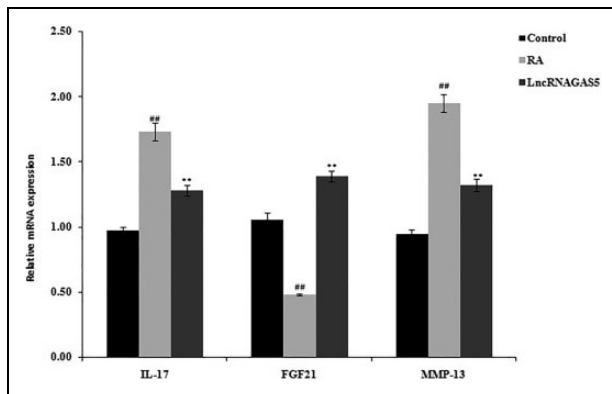


Figure 5. Effect of LncRNA-GAS5 siRNA on the levels of cartilage mRNAs encoding FGF21, MMP-13, and IL-17 (qRT-PCR assay). Mean \pm SEM (n = 10); ###P < .01 compared to the control group; **P < .01 compared to the RA group. FGF indicates fibroblast growth factor; GAS5, growth arrest-specific transcript 5; LncRNA, long noncoding RNA; MMP, matrix metalloproteinases; RA, rheumatoid arthritis; qRT-PCR, quantitative real-time polymerase chain reaction; siRNA, small interfering RNA.

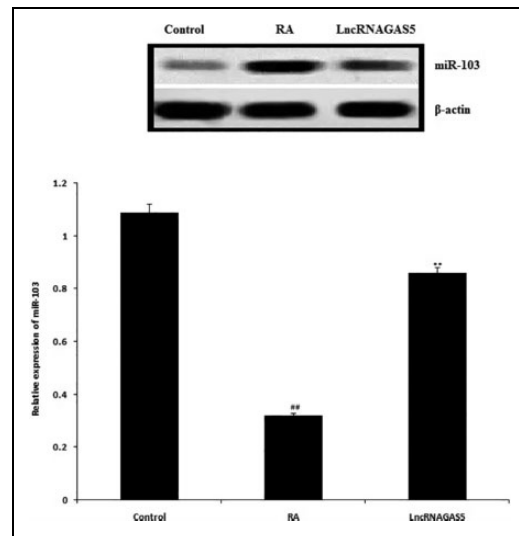


Figure 7. Effect of LncRNA-GAS5 siRNA on cartilage miR-103 expression. Mean \pm SEM (n = 10); ###P < .01 compared to the control group; **P < .01 compared to the RA group. GAS5 indicates growth arrest-specific transcript 5; LncRNA, long noncoding RNA; siRNA, small interfering RNA.

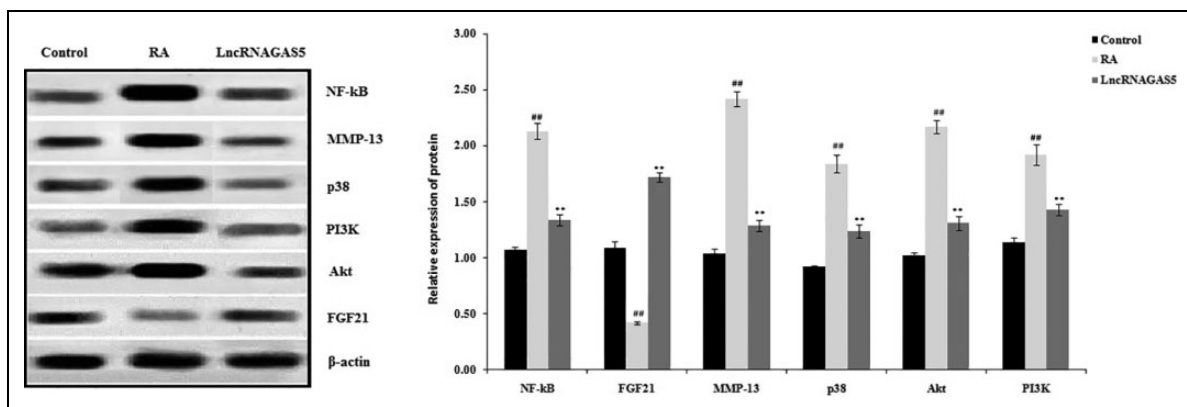


Figure 6. Effect of LncRNA-GAS5 siRNA on the expression levels of cartilage MMP-13, NF- κ B, FGF21, p38, Akt, and PI3K (Western blot assay). Mean \pm SEM (n = 10); ###P < .01 compared to the control group; **P < .01 compared to the RA group. FGF indicates fibroblast growth factor; GAS5, growth arrest-specific transcript 5; LncRNA, long noncoding RNA; MMP, matrix metalloproteinases; RA, rheumatoid arthritis; siRNA, small interfering RNA.

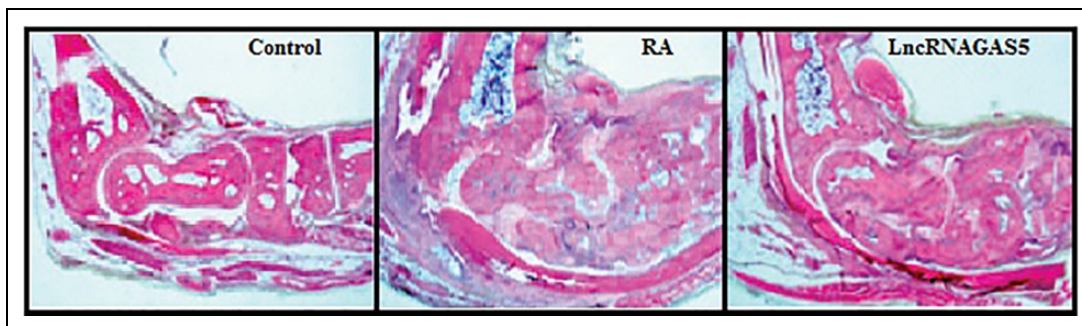


Figure 8. Effect of LncRNA-GAS5 siRNA on the histopathology of cartilage tissue. GAS5 indicates growth arrest-specific transcript 5; LncRNA, long noncoding RNA; siRNA, small interfering RNA.

adipose tissue is converted into brown adipose tissue, increasing the cytokine levels and predisposing such subjects to RA.¹⁹ We thus induced RA in obese mice. The levels of serum cytokines; oxidative stress markers; biochemical lipid parameters; and AST, ALT, and CRP changed in RA mice; LncRNA-GAS5 siRNA normalized all of these alterations.

Autoimmune disorders, including RA, are associated with increased expression of PI3K and Akt; several drugs seek to reduce these rises.²⁰ Matrix metalloproteinases-13 expression is regulated by both PI3K and Akt via changes in the levels of inflammatory cytokines that maintain synovial fibroblast numbers.²¹ Matrix metalloproteinases-13 expression is enhanced in RA patients, in turn reducing cartilage FGF21 expression, triggering cartilage destruction.²² We found that LncRNA-GAS5 siRNA normalized cartilage MMP-13, PI3K, Akt, FGF21, IL-17, and NF- κ B expression. Also, histology showed that LncRNA-GAS5 siRNA protected against the development of pathological cartilage changes. Increased miR-103 expression aggravates inflammatory disorders, including RA.²³ miR-103 modulates PI3K and Akt expression, enhancing chondrocyte apoptosis; inhibition of such apoptosis protects against RA. Long noncoding RNA-GAS5 siRNA reduced cartilage miR-103 expression compared to that in RA mice.

Conclusion

Long noncoding RNA-GAS5 protects the cartilage of RA mice by modulating the PI3K/Akt/FGF21 pathway via inhibition of miR-103 expression.

Authors' Note

Hongwei Chen and Chuan He are authors contribute to this work equally. The English in this document has been checked by at least two professional editors, both native speakers of English. For a certificate, please see: <http://www.textcheck.com/certificate/MSI9dh>

Acknowledgment

The authors thank the Jingzhou Traditional Chinese Medicine Hospital, China, for facilitating our work.


Declaration of Conflicting Interests

The author(s) declared no potential conflicts of interest with respect to the research, authorship, and/or publication of this article.

Funding

The author(s) disclosed receipt of the following financial support for the research, authorship, and/or publication of this article: There is no external funding for presented protocol, and Jingzhou Traditional Chinese Medicine Hospital, China, provided necessary facility to conduct the presented work.

ORCID iD

Qixiong Pang  <https://orcid.org/0000-0003-3447-1495>

References

- Kim Y, Oh HC, Park JW, et al. Diagnosis and treatment of inflammatory joint disease. *Hip Pelvis*. 2017;29(4):211-222.
- Maldonado M, Nam J. The role of changes in extracellular matrix of cartilage in the presence of inflammation on the pathology of osteoarthritis. *Biomed Res Int*. 2013;2013:284873.
- Yap HY, Tee SZ, Wong MM, Chow SK, Peh SC, Teow SY. Pathogenic role of immune cells in rheumatoid arthritis: implications in clinical treatment and biomarker development. *Cells*. 2018;7(10):161.
- Cekici A, Kantarci A, Hasturk H, Van Dyke TE. Inflammatory and immune pathways in the pathogenesis of periodontal disease. *Periodontol 2000*. 2014;64(1):57-80.
- Corrado A, Maruotti N, Cantatore FP. Osteoblast role in rheumatic diseases. *Int J Mol Sci*. 2017;18(6):1272.
- Abdulkhaleq LA, Assi MA, Abdullah R, Zamri-Saad M, Taufiq-Yap YH, Hezmee MNM. The crucial roles of inflammatory mediators in inflammation: a review. *Vet World*. 2018;11(5):627-635.
- Schmidt FM, Weschenfelder J, Sander C, et al. Inflammatory cytokines in general and central obesity and modulating effects of physical activity. *PLoS One*. 2015;10(3):e0121971.
- Townsend K, Tseng YH. Brown adipose tissue: recent insights into development, metabolic function and therapeutic potential. *Adipocyte*. 2012;1(1):13-24.
- Chen TM, Chen YH, Sun HS, Tsai SJ. Fibroblast growth factors: potential novel targets for regenerative therapy of osteoarthritis. *Chin J Physiol*. 2019;62(1):2-10.

10. Ji J, Dai X, Yeung SJ, He X. The role of long non-coding RNA GAS5 in cancers. *Cancer Manag Res.* 2019;11:2729-2737.
11. Dong Z, Li S, Wang X, et al. lncRNA GAS5 restrains CCl₄-induced hepatic fibrosis by targeting miR-23a through the PTEN/PI3K/Akt signaling pathway. *Am J Physiol Gastrointest Liver Physiol.* 2019;316(4):G539-G550.
12. Lu S, Su Z, Fu W, Cui Z, Jiang X, Tai S. Altered expression of long non-coding RNA GAS5 in digestive tumors. *Biosci Rep.* 2019;39(1):BSR20180789.
13. Yu XM, Meng HY, Yuan XL, et al. MicroRNAs' involvement in osteoarthritis and the prospects for treatments. *Evid Based Complement Alternat Med.* 2015;236179.
14. Liu YL, Lin HM, Zou R, et al. Suppression of complete Freund's adjuvant-induced adjuvant arthritis by cobra toxin. *Acta Pharmacol Sin.* 2009;30(2):219-227.
15. Guo Q, Wang Y, Xu D, Nossent J, Pavlos NJ, Xu J. Rheumatoid arthritis: pathological mechanisms and modern pharmacologic therapies. *Bone Res.* 2018;6:15.
16. Rachchh RP, Galani VJ. Evaluation of antinociceptive and anti-rheumatic activity of *Grangea maderaspatana* (L.) Poir. using experimental models. *Ayu.* 2015;36(4):425-431.
17. Hayer S, Bauer G, Willburger M, et al. Cartilage damage and bone erosion are more prominent determinants of functional impairment in longstanding experimental arthritis than synovial inflammation. *Dis Model Mech.* 2016;9(11):1329-1338.
18. Mateen S, Moin S, Shahzad S, Khan AQ. Level of inflammatory cytokines in rheumatoid arthritis patients: correlation with 25-hydroxy vitamin D and reactive oxygen species. *PLoS One.* 2017;12(6):e0178879.
19. Gómez-Hernández A, Beneit N, Díaz-Castroverde S, Escribano Ó. Differential role of adipose tissues in obesity and related metabolic and vascular complications. *Int J Endocrinol.* 2016;1216783.
20. Stark AK, Sriskantharajah S, Hessel EM, Okkenhaug K. PI3 K inhibitors in inflammation, autoimmunity and cancer. *Curr Opin Pharmacol.* 2015;23:82-91.
21. Bustamante MF, Garcia-Carbonell R, Whisenant KD, Guma M. Fibroblast-like synoviocyte metabolism in the pathogenesis of rheumatoid arthritis. *Arthritis Res Ther.* 2017;19(1):110.
22. Yu Y, Li S, Liu Y, et al. Fibroblast growth factor 21 (FGF21) ameliorates collagen-induced arthritis through modulating oxidative stress and suppressing nuclear factor-kappa B pathway. *Int Immunopharmacol.* 2015;25(1):74-82.
23. Tahamtan A, Teymoori-Rad M, Nakstad B, Salimi V. Anti-inflammatory microRNAs and their potential for inflammatory diseases treatment. *Front Immunol.* 2018;9:1377.